Citation: Cell Death and Disease (2012) 3, e312; doi:10.1038/cddis.2012.46

www.nature.com/cddis

Impaired mitochondrial biogenesis contributes to depletion of functional mitochondria in chronic MPP^+ toxicity: dual roles for ERK1/2

JH Zhu[1], AM Gusdon[1], H Cimen[2], B Van Houten[3], E Koc[4] and CT Chu*[,1,5,6]

The regulation of mitochondrial quality has emerged as a central issue in neurodegeneration, diabetes, and cancer. We utilized repeated low-dose applications of the complex I inhibitor 1-methyl-4-phenylpyridinium (MPP^+) over 2 weeks to study cellular responses to chronic mitochondrial stress. Chronic MPP^+ triggered depletion of functional mitochondria resulting in diminished capacities for aerobic respiration. Inhibiting autophagy/mitophagy only partially restored mitochondrial content. In contrast, inhibiting activation of extracellular signal-regulated protein kinases conferred complete cytoprotection with full restoration of mitochondrial functional and morphological parameters, enhancing spare respiratory capacity in MPP^+ co-treated cells above that of control cells. Reversal of mitochondrial injury occurred when U0126 was added 1 week after MPP^+, implicating enhanced repair mechanisms. Chronic MPP^+ caused a $>90\%$ decrease in complex I subunits, along with decreases in complex III and IV subunits. Decreases in respiratory complex subunits were reversed by co-treatment with U0126, ERK1/2 RNAi or transfection of dominant-negative MEK1, but only partially restored by degradation inhibitors. Chronic MPP^+ also suppressed the *de novo* synthesis of mitochondrial DNA-encoded proteins, accompanied by decreased expression of the mitochondrial transcription factor TFAM. U0126 completely reversed each of these deficits in mitochondrial translation and protein expression. These data indicate a key, limiting role for mitochondrial biogenesis in determining the outcome of injuries associated with elevated mitophagy.

Cell Death and Disease (2012) **3,** e312; doi:10.1038/cddis.2012.46; published online 24 May 2012
Subject Category: Neuroscience

Mitochondrial dysfunction has long been implicated in Parkinson's disease (PD) pathogenesis.[1] Reduced mitochondrial complex I activity is observed in the substantia nigra of patients with PD. Neurotoxins, such as rotenone or 1-methyl-4-phenylpyridinium (MPP^+), which inhibit complex I of the mitochondrial respiratory chain, cause degeneration of dopaminergic neurons. Recently, diverse proteins involved in familial PD, including α-synuclein, Parkin, DJ-1, and PTEN-induced kinase 1, have been implicated in regulating mitochondrial dynamics and quality control.[1]

A key element in mitochondrial quality control involves autophagic targeting of mitochondria for lysosomal degradation. Recent studies implicate induction of the autophagy-lysosome pathway in genetic and toxin models of PD.[2–5] Decreases in chaperone-mediated autophagy,[6] elicit further increases in macroautophagy (hereafter autophagy), but this compensatory increase may ultimately prove detrimental.[7] Although autophagosomes are observed in substantia nigra neurons of PD and Lewy body dementia patients,[8,9] whether autophagy is protective or detrimental may depend on interactions of this pathway with other metabolic or reparative pathways.

We previously demonstrated that acute MPP^+ or 6-hydroxydopamine (6-OHDA) treatments induce autophagy and mitochondrial degradation in SH-SY5Y cells, mediated by activation of extracellular signal-regulated protein kinases (ERK).[2,4] Given that chronic or repetitive micro-insults have been proposed as possible contributing factors for human neurodegenerative diseases,[10] and chronic PD models may

[1]Department of Pathology, Division of Neuropathology, University of Pittsburgh School of Medicine, Pittsburgh, PA 15213, USA; [2]Department of Biochemistry and Molecular Biology, Pennsylvania State University, University Park, PA 16802, USA; [3]The Department of Pharmacology and Chemical Biology, University of Pittsburgh Cancer Institute, University of Pittsburgh School of Medicine, Pittsburgh, PA 15213, USA; [4]Department of Biochemistry & Microbiology, Marshall University, Huntington, WV 25701, USA; [5]The McGowan Institute for Regenerative Medicine, University of Pittsburgh School of Medicine, Pittsburgh, PA 15213, USA and [6]The Center for Neuroscience, University of Pittsburgh, Pittsburgh, PA 15213, USA
*Corresponding author: Charleen T Chu, Department of Pathology/Division of Neuropathology, University of Pittsburgh School of Medicine, 200 Lothrop St, Pittsburgh, PA 15213, USA. Tel: 412 383 5379; E-mail: ctc4@pitt.edu
Keywords: Parkinson's disease; 1-methyl-4-phenyl-1,2,3,6-tetrahydropyridine; autophagy; mitochondrial biogenesis; mitogen-activated protein kinases; mitochondrial transcription factor A
Abbreviations: Atg7, Autophagy-related protein 7; AVs, autophagic vacuoles; DAT, dopamine transporter; ERK, extracellular signal-regulated protein kinase; FCCP, carbonylcyanide-p-trifluoromethoxyphenylhydrazone; 6-OHDA, 6-hydroxydopamine; LC3, microtubule-associated protein 1 light chain 3 (Atg8); MEK1/2, mitogen-activated protein (MAP) kinase kinase 1/2; MPP^+, 1-methyl-4-phenylpyridinium; NDUFA9, NADH-ubiquinone oxidoreductase alpha subunit 9; NRF-1, nuclear respiratory factor 1; OCR, oxygen consumption rate; OXPHOS, oxidative phosphorylation; PDH, Pyruvate dehydrogenase; PGC-1α, Peroxisome proliferator-activated receptor gamma coactivator 1-alpha; RA, retinoic acid; RC, reserve capacity or spare respiratory capacity of mitochondria; ROS, reactive oxygen species; siRNA, small interfering RNA; siCtrl, non-targeting control siRNA; TFAM, mitochondrial transcription factor A; U0126, 1,4-diamino-2,3-dicyano-1,4-bis[2-aminophenylthio] butadiene; VMAT2, vesicular monoamine transporter 2
Received 13.10.11; revised 12.3.12; accepted 30.3.12; Edited by P Salomoni

more fully mimic α–synuclein aggregation and formation of Lewy body-like structures,[11,12] we modified our MPP$^+$ injury model to cause gradual cell death over a 2-week period to study the potential roles of compensatory or repair pathways.

Retinoic acid-differentiated SH-SY5Y cells were treated with multiple low doses of MPP$^+$, resulting in striking changes in mitochondrial morphology, function and autophagy, with depletion of nuclear DNA-encoded mitochondrial proteins and impaired translation of mitochondrial DNA (mtDNA)-encoded proteins. Similar to the acute model, inhibition of autophagy using siRNA to the essential autophagy proteins Atg7 or microtubule-associated protein 1 light chain 3 (LC3) conferred partial protection against autophagic cell death. In contrast to the acute model, however, the MPP$^+$-induced disruption in mitochondrial morphology, protein expression, and function was completely reversed by inhibition of ERK1/2 activation. These data suggest that in the chronic setting, blunting the rapid mitochondrial turnover induced by MPP$^+$ serves to prevent autophagic cell death, while allowing compensatory/reparative biogenesis responses to develop.

Results

Characterization of a 2-week model of progressive MPP$^+$ toxicity. Retinoic acid-differentiated SH-SY5Y cells were treated with lower doses of MPP$^+$ (in fresh medium) three times a week, resulting in time- and dose-related neuronal cell death over 2 weeks (Supplementary Figure S1A). Chronic MPP$^+$ treatment caused fragmentation of the reticular mitochondrial network observed in control cells, with isolated, sometimes enlarged, mitochondria (Figure 4b), reductions in mitochondrial membrane potential (Supplementary Figure S1B), and numerous ultrastructural alterations (Figure 4d). The mitochondrial matrix was pale with disorganized cristae often restricted to the periphery. Quantitative ultrastructural analysis revealed significant increases in the percentage of both the smallest ($\leq 0.2\,\mu m^2$) and largest ($>3.0\,\mu m^2$) mitochondrial profiles, with increased circularity of those $>1\,\mu m^2$ of area, consistent with swelling (Supplementary Figures S1C–E).

Chronic MPP$^+$ increased autophagic flux in SH-SY5Y cells. GFP-LC3 is an established marker of pre-autophagosomal membranes (phagophores) and early autophagic vacuoles (AVs). In stable GFP-LC3-expressing, neuronal-differentiated SH-SY5Y cells, chronic MPP$^+$ treatment led to a reduction in very fine GFP-LC3 granules and an increase in coarse GFP-LC3 puncta, often with ring-like morphology (Figures 1a–c). Ultrastructural analysis confirmed increased AVs in the cell body and in neurites (Figures 1d–f). Chronic MPP$^+$ treatment also significantly increased the average

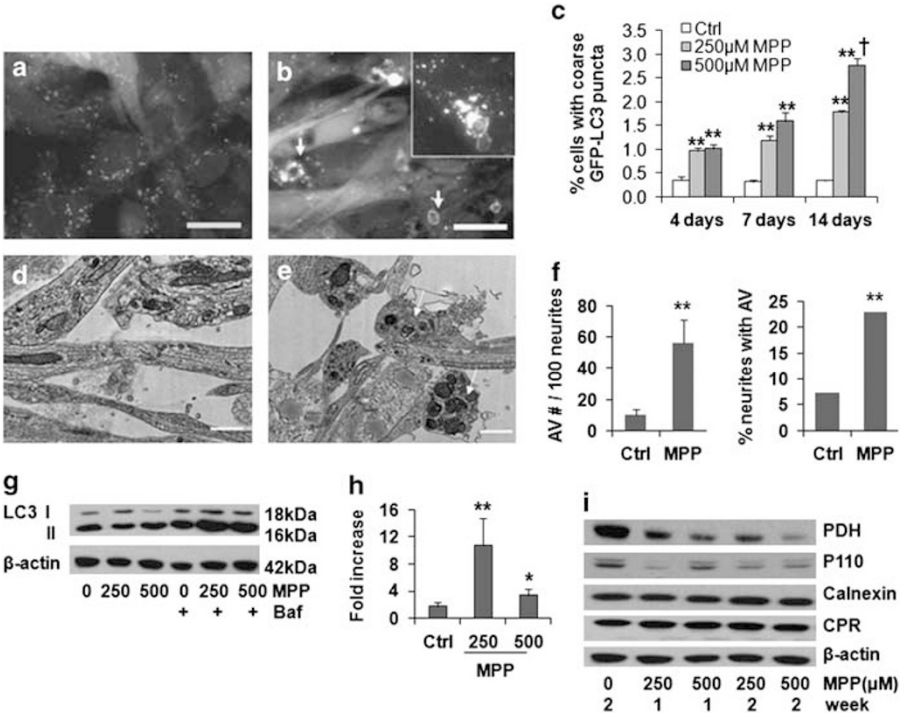

Figure 1 Selective mitophagy is induced in the 2-week MPP$^+$ model. MPP$^+$ treatment (250 μM) $\times$ 2 weeks induced formation of enlarged, coarse GFP-LC3 puncta, some displaying ring-like or bead-like morphology (**b**, arrows), compared with control (**a**). Autophagic puncta were also identified by immunostaining for endogenous LC3 (**b**, inset) (scale bar = 20 μm). There were significant time- and dose-related increases in coarse GFP-LC3 puncta (**c**). $^{**}P<0.01$ MPP$^+$ *versus* Ctrl. $^{\dagger}P<0.01$ 500 μM *versus* 250 μM. Electron microscopy revealed increased autolysosomal structures in neurites after MPP$^+$ treatment (**e**) compared with control neurites (**d**) (scale bar = 1 μm), quantified as increases in either the number of AVs in neurites or the number of neurites containing AVs (**f**) $^{**}P<0.01$, MPP$^+$ *versus* control, *t*-test, and chi-square test, respectively). Representative LC3 western blot shows increased LC3 II elicited by MPP$^+$ in the presence of bafilomycin, added during the final 24 h to prevent degradation of newly formed AVs (**g**), and flux analysis using the change in LC3 II/actin ratios in the presence *versus* absence of bafilomycin confirmed a significant increase, particularly at the lower dose (**h**, $n=3$). $^{**}P<0.01$, $^{*}P<0.05$, MPP$^+$ *versus* Ctrl. Western blot showed mitochondrial protein loss (PDH, P110), with no change in endoplasmic reticulum proteins cytochrome p450 reductase (CPR) or calnexin (**i**)

size of monodansylcadavarine fluorescent puncta (Supplementary Figures S2A and B), consistent with fusion and maturation to autolysosomes.

Treatment with bafilomycin A1, an inhibitor of early AV acidification and fusion to lysosomes, was used to arrest degradation of LC3 II, the form of LC3 that is covalently bound to autophagic membranes. The difference in LC3 II levels in the presence and absence of bafilomycin reflects the degradative flux of autophagosomes in that time frame.[13] In contrast to acute MPP$^+$ toxicity, chronic MPP$^+$ caused a slight decrease in the steady-state LC3 II level. As reported in other cell types, induction of autophagy can cause a decrease in LC3 II levels due to increased turnover of LC3 protein.[13] The addition of bafilomycin A1 to MPP$^+$-treated cells caused a greater increase in LC3 II levels than that observed in control cells, indicating an increase in LC3 turnover in cells treated chronically with MPP$^+$, particularly at the lower dose (Figures 1g and h). There was mitochondrial protein loss, but no marked change in two endoplasmic reticulum proteins (Figure 1i), indicating induction of selective mitophagy.

Autophagy does not have a major, determining role for cell fate during chronic MPP$^+$ toxicity. In the acute MPP$^+$ model, inhibition of autophagy does not prevent mitochondrial damage, but reduces autophagic cell death.[4] In the chronic model, RNAi of Atg7 or LC3 attenuated the increase in LC3 II and reduced the number of autophagic vacuoles (Figures 2a and b), but resulted in only modest protection (Supplementary Figure S2C). Interestingly, Atg7 knockdown protected MPP$^+$-treated cells against mitochondrial swelling (Figure 2b), inhibited the loss of mitochondrial protein p60 and PDH (Figure 2c; Supplementary Figure S2D) and conferred partial improvement in maximal oxygen consumption rates (OCR) (Figure 2d), which were not observed in the acute model.[4] These data suggest that limiting the autophagic response may unmask other compensatory responses in the chronic MPP$^+$ model.

Inhibition of ERK1/2 activation reversed structural damage to mitochondria and preserved levels of mitochondrial complex proteins in chronic MPP$^+$-treated cells. ERK1/2 has been implicated in the regulation of autophagy and mitophagy,[2,4,14] showing a time-related 40–50% increase, peaking and then decreasing after each MPP$^+$ pulse (Figures 3a and b). Increased ERK1/2 activity was observed using an *in vitro* kinase pull-down assay (Figure 3c) and a luciferase assay detecting the *in situ* activity of transfected ERK2 or its kinase-dead control (Figure 3d).

Inhibiting the upstream MAPK/ERK1/2 kinase (MEK) by adding U0126 with each dose of MPP$^+$ conferred nearly complete protection against MPP$^+$-induced cell death (Figure 4a). This protection was not due to decreased expression of dopamine transporter, increased expression of vesicular monoamine transporter, or interference with the acute effects of MPP$^+$ on mitochondrial respiration (Supplementary Figures S3A and B). Instead, U0126 reversed the mitochondrial morphology changes (Figure 4b) and the loss of mitochondrial proteins (Figure 4c; Figure 5c) observed in cells chronically

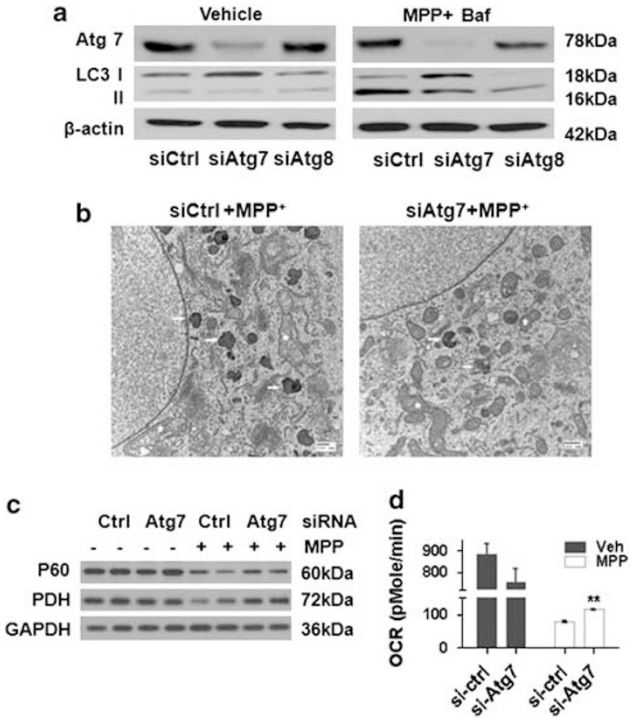

Figure 2 Inhibiting autophagy conferred partial protection in the 2-week MPP$^+$ model. Either Atg7 or Atg8 (LC3B) siRNA reduced the LC3 II increase elicited by MPP$^+$ (250 μM $\times$ 10 days with 10 nM bafilomycin for the last 4 h) (**a**). Electron microscopy confirmed reduced AVs (arrows) in Atg7 siRNA and MPP$^+$ co-treated cells (**b**, 250 μM $\times$ 10 days) compared with MPP$^+$-treated cells. Improvement of mitochondrial morphology was also observed (**b**, star). Atg7 protein knockdown ameliorated MPP$^+$-induced reductions of mitochondrial protein p60 and PDH (**c**; see Supplementary Figure S2D for densitometry), with a modest recovery in FCCP-elicited maximal OCR in Atg7 siRNA knockdown cells compared with control siRNA-treated cells (**$P<0.01$ *versus* si-ctrl) (**d**)

stressed with MPP$^+$. U0126/MPP$^+$ co-treated cells displayed relatively uniform mitochondria with intact inner and outer membranes and preserved cristae (Figure 4d). The degree of protection was much greater than that observed by inhibiting autophagy alone, implicating other mechanisms to promote the integrity of chronically injured mitochondria.

MPP$^+$ can directly inhibit complex I (NADH-ubiquinone oxidoreductase) activity of the mitochondrial electron transport chain although other mechanisms of toxicity have also been implicated.[15] MPP$^+$ caused $>90\%$ decrease in the nuclear-encoded alpha subunit 9 (NDUFA9), with complete reversal by U0126 (Figures 5a and b). Similar results were observed for the complex I subunit NDUFB8 and for proteins in complex IV (Figure 5c), with a lesser effect on complex III and no effect on complex V-alpha. The decreased respiratory protein expression could be partially attributed to the combined activities of the proteasome, autophagy-lysosome system and the mitochondrial LON peptidase 1 (Supplementary Figures S3C–F). As the U0126 data implicated the MEK/ERK signaling pathway, we transfected SH-SY5Y cells with either siRNA targeting ERK1/2 (Figure 5g; Supplementary Figure S3G) or dominant-negative MEK1 (DN-MEK1; Supplementary Figures S4A and B).

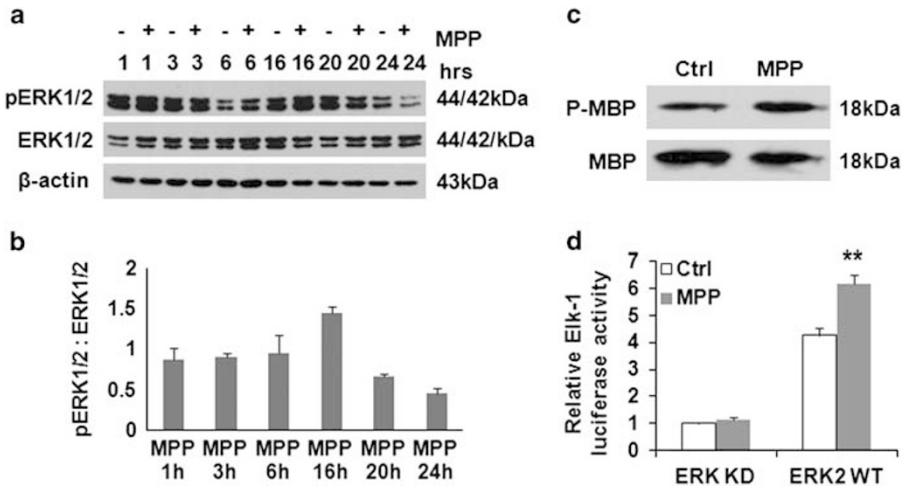

Figure 3 Chronic MPP^+ treatment increased ERK1/2 activity. A time-related increase of ERK1/2 phosphorylation was observed by 16 h after each pulse of 250 μM MPP^+ (**a** and **b**). ERK1/2 immunoprecipitated from control and MPP^+-treated cells were analyzed for activity in phosphorylating myelin basic protein (MBP) (**c**). Intracellular ERK activation was measured using the Elk1 trans-Reporting System (**d**) in cells transfected with wild-type (WT) or kinase-deficient (KD) ERK2. $^{**}P<0.01$, ERK2-WT (MPP^+ *versus* Ctrl)

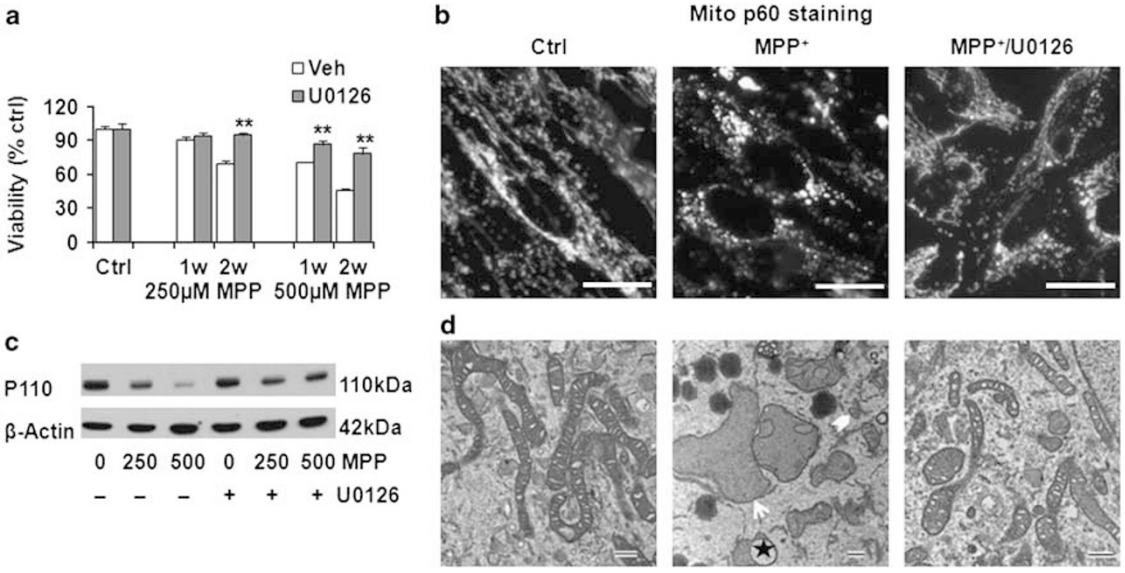

Figure 4 Inhibiting ERK1/2 activation protects against cell death and restores mitochondrial morphology. The MEK inhibitor U0126 restored the viability of cells treated with MPP^+ (**a**); prevented MPP^+-induced mitochondrial fragmentation, formation of giant mitochondria, and disruption of mitochondrial interconnectivity (**b**, 250 μM MPP^+, 2 weeks; immunostain for mitochondrial protein p60; scale bar = 20 μm); and reduced chronic MPP^+-induced mitochondrial protein P110 loss (**c**). Compared with control mitochondria, 250 μM MPP^+ × 2 weeks caused loss, disarray, and disruption of mitochondrial cristae (**d**). Many mitochondrial profiles are small and fragmentated (chevron) but some become giant or swollen (arrow), showing evagination (star). Co-treatment with MPP^+ and U0126 reversed these changes (**d**, scale bar: 500 nm). $^{**}P<0.01$, $U0126^+$ *versus* Veh

Either of these methods also attenuated the MPP^+-elicited decrease in mitochondrial respiratory complex proteins.

Amelioration of MPP^+ induced structural changes is associated with restoration of basal function and enhanced spare respiratory capacity. Analysis of live cell aerobic respiration revealed that U0126 not only reversed the MPP^+-induced decrease in basal respiration (the mean of the first four time points in Figure 5d), but also caused a further increase in FCCP-induced maximal mitochondrial respiration (Figures 5d and e). If cells were cultured in galactose for 24 h prior to analysis to induce dependence on mitochondrial respiration,[16] MPP^+ reduced cellular ATP concentrations, and this effect was also rescued by U0126 (Figure 5f). Moreover, the spare respiratory capacity[17] or mitochondrial reserve capacity (RC), defined as the difference between maximal FCCP-induced respiration and basal respiration, was increased above the baseline control cell level by approximately six-fold in MPP^+-injured cells rescued by U0126 (Figure 5e).

To distinguish prevention of injury from enhanced compensation or recovery, we conducted experiments in which the MEK1/2 inhibitor was added 1 week after beginning MPP^+

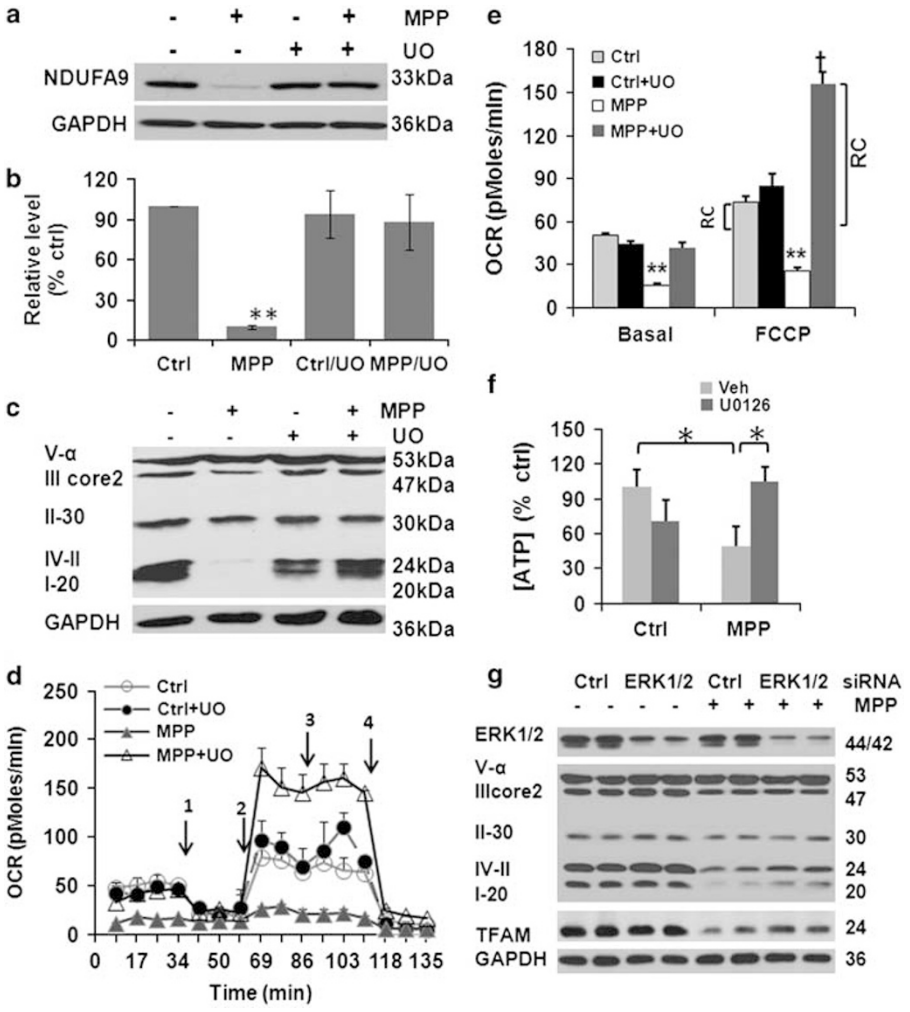

Figure 5 Inhibiting ERK1/2 activation restores respiratory complex protein expression and function. A significant decrease of NDUFA9 protein was observed in cells with 250 μM MPP$^+$ $\times$ 2 weeks, which was prevented by 5 μM U0126 (**a**, **b**, $n=4$). $^{**}P<0.01$, MPP$^+$ *versus* ctrl, ctrl + U0126, and MPP$^+$/U0126. The complex I subunit NDUFB8, complex IV-cytochrome oxidase subunit II and complex III core 2 were also decreased with MPP$^+$, and restored by co-treatment with U0126 (**c**). Mitochondrial oxygen consumption was analyzed using an XF24 Extracellular Flux Analyzer. Oxygen consumption rate (OCR) curves are shown under basal conditions (**d**) and after addition of 1 μM oligomycin (D-1), 300 nM FCCP (D-2), 120 mM 2-DG (D-3), and 1 μM rotenone (D-4). MPP$^+$ caused significant decrease of basal (before 1) and maximal (between 2 and 3) FCCP-induced OCR. U0126 not only reversed the MPP$^+$-induced OCR inhibition, but also increased mitochondrial reserve capacity (RC) beyond that of control cells (**e**). $^{**}P<0.01$ MPP$^+$ *versus* Ctrl, ctrl + U0126, and MPP$^+$ + U0126; $^{\dagger}P<0.01$ MPP$^+$ + U0126 *versus* ctrl or ctrl + U0126. Cells were shifted into galactose as a fuel source for 24 h to stimulate dependence on mitochondrial respiration. Under this condition, MPP$^+$ elicited a reduction in ATP levels that was reversed by concurrent treatment with U0126. $^{*}P<0.05$ as indicated (**f**). RNAi-mediated knockdown of ERK1/2 also diminished the decrease in TFAM, complex I and IV subunits that were elicited by MPP$^+$ (250 μM, 2 weeks) (**g**; Supplementary Figure S3G for densitometry)

treatments (Supplementary Figures S4C–F). At 1 week, there are already significant alterations in mitochondrial structure and function. Addition of U0126 during the second week of continued MPP$^+$ treatments significantly restored mitochondrial structure and function (Supplementary Figure S4F), implicating the involvement of reparative pathways.

Inhibiting MEK/ERK activation restores indices of mitochondrial biogenesis in MPP$^+$-treated cells. Peroxisome proliferator-activated receptor gamma coactivator 1-alpha (PGC-1α), nuclear respiratory factor 1 (NRF-1), and mitochondrial transcription factor A (TFAM) regulate mitochondrial biogenesis. Whereas the former two factors act as co-regulators of nuclear transcription, PGC-1α also functions in the mitochondria,[18] and TFAM has an important role in mtDNA stability and the biosynthesis of the 13 mtDNA-encoded respiratory chain subunits.

There were no significant changes in the levels of PGC-1α or NRF-1 (Figure 6a; Supplementary Figures S5A and B), although subcellular localization of PGC-1α was altered. In control cells, PGC-1α was colocalized with mitochondrial marker p60, as described in other systems.[18] Significant nuclear signal was not observed, consistent with its constitutive nuclear export unless phosphorylated.[19] MPP$^+$ elicited dissociation of cytoplasmic PGC-1α granules from mitochondria (Figures 6b and c; Supplementary Figure S5C), which was opposed by U0126. There were no significant changes in PGC-1α mRNA levels (Supplementary Figure S5D).

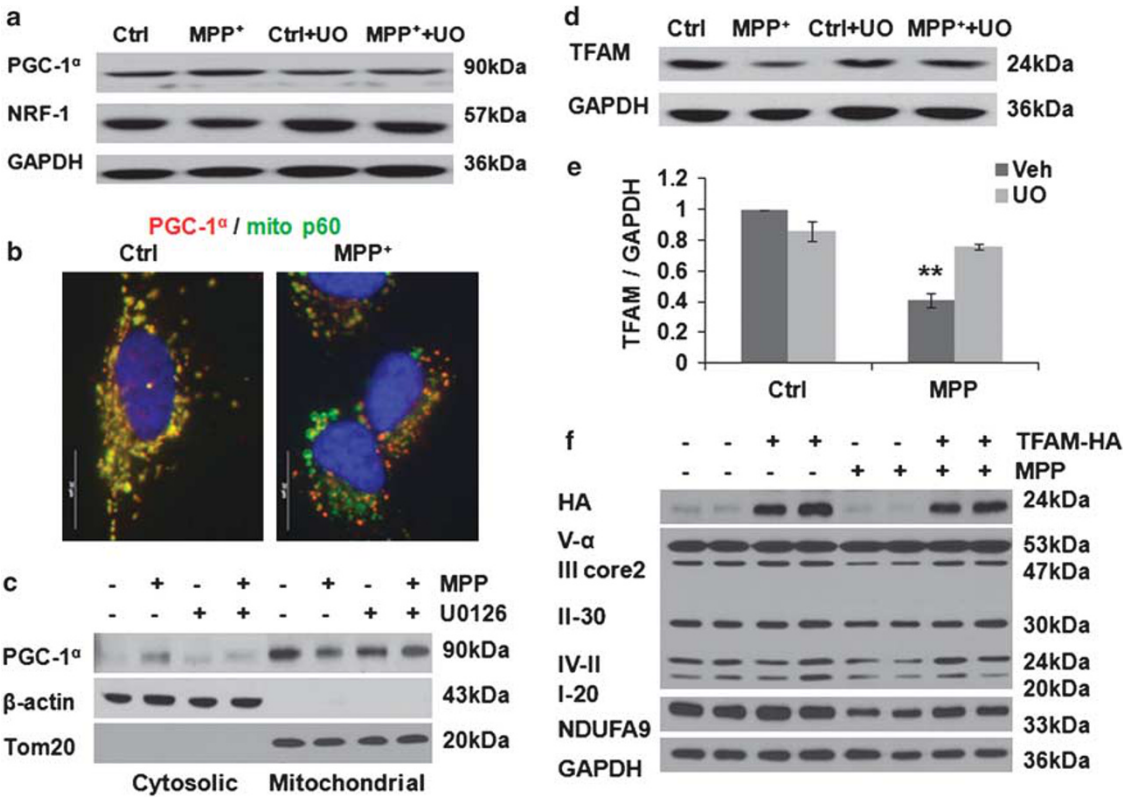

Figure 6 Effects of chronic MPP^+ on mitochondrial biogenesis proteins. MPP^+ treatment (250 μM, 2 weeks) did not significantly change the total PGC-1α and NRF-1 protein levels (**a**); however, MPP^+ caused a loss of PGC-1α granules from mitochondria by double immunostaining (**b**, scale bar: 20 μm; Supplementary Figure S5C). Relocation of PGC-1α from mitochondria to cytosol was further studied by western blot of mitochondrial and cytosolic fractions prepared using the FOCUS SubCell kit (G-Biosciences, St Louis, MO, USA) (**c**). TFAM was significantly decreased after MPP^+ treatment, prevented by U0126 (**d** and **e**). $^{**}P<0.01$ MPP^+ *versus* Ctrl, Ctrl + U0126, and MPP^+ + U0126, $n=4$ for (**e**). Overexpression of TFAM restored the expression levels of complex I (NDUFA9), III core2, and IV-II subunits in MPP^+-injured cells (**f**; Supplementary Figure S5E for densitometry)

In contrast, TFAM protein was significantly decreased after chronic MPP^+ treatment (Figures 6d and e). TFAM mRNA levels were not significantly decreased (Supplementary Figure S5D), whereas inhibition of the mitochondrial Lon peptidase 1 produced restoration of TFAM levels in MPP^+-treated cells (Supplementary Figure S3F), implicating a degradative process. As mitochondrially localized PGC-1α binds the D-loop region of mtDNA, where it interacts with TFAM,[18] and TFAM is central to transcription of mitochondrial genes, we directly studied mitochondrial protein synthesis by [^{35}S]-methionine pulse labeling. Whereas a single dose of 250 μM MPP^+ had little effect on mitochondrial translation, chronic administration of MPP^+ over 1 week significantly inhibited biosynthesis of the 13 mtDNA-encoded respiratory chain subunits (Figures 7a and c). However, it has no apparent effect on nuclear DNA-encoded protein translation (Figure 7b). The MEK inhibitor U0126 prevented the decrease in TFAM protein levels in MPP^+-treated cells (Figures 6d and e), and restored translation of the mtDNA-encoded proteins (Figures 7a and c). ERK1/2 siRNA protected TFAM levels in MPP^+-treated cells (Figure 5g; Supplementary Figure S3G). Furthermore, overexpression of TFAM-HA reversed MPP^+-induced decreases in respiratory complex I, III, and IV subunits (Figure 6f, Supplementary Figure S5E).

Discussion

Low dose, repeated MPP^+ administration caused significant loss of functional mitochondria, accompanied by increased mitophagy, alterations in nuclear-encoded biogenesis proteins and suppression of mitochondrial translation. While suppressing autophagy conferred only partial restoration of mitochondrial content, the MEK inhibitor U0126 conferred complete restoration of mitochondrial protein content, morphology, and function. Similar protective effects were observed after use of ERK1/2 siRNA or DN-MEK1 to downregulate the ERK1/2 signaling pathway. These changes were accompanied by recovery of TFAM levels and restored translation of mtDNA-encoded respiratory subunits, indicating that suppression of mitochondrial biogenesis has an important role in the loss of mitochondrial function accompanying chronic, low-dose exposures to MPP^+.

Mitochondrial respiration is tightly linked to ATP production. Neurons and differentiated neuronal cells are largely dependent upon oxidative phosphorylation and usually exhibit a substantial mitochondrial RC (also known as spare respiratory capacity), to rapidly meet the requirements of increased functional demand and stress.[17] Indeed, the RC is a major determinant of the outcome of neuronal excitotoxicity,

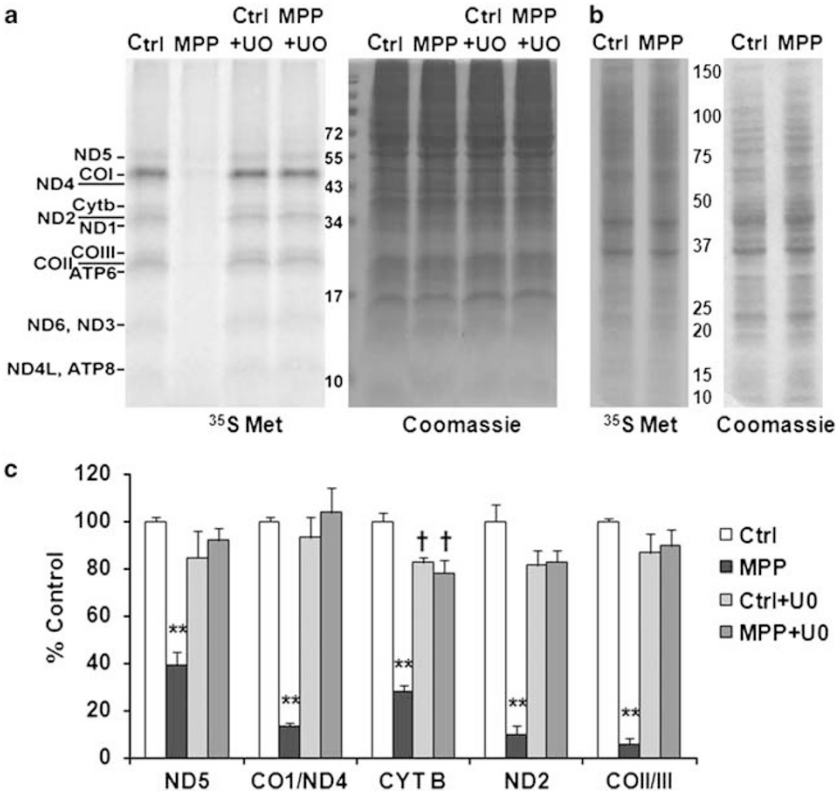

Figure 7 MPP+ inhibits synthesis of mtDNA-encoded respiratory subunits, restored by U0126. A representative autoradiogram showed that MPP+ treatment for 1 week caused marked decreases in newly synthesized ^{35}S-Met-labeled mtDNA-encoded translation products, reversed by co-treatment with U0126 (**a**). In contrast, overall protein translation levels assessed in the absence of emetine revealed no obvious effects on total (predominantly nuclear-encoded) protein synthesis (**b**). The graph (**c**) is a quantification of three independent pulse-labeling experiments normalized by Coomassie Brilliant Blue stain. $^{**}P<0.01$ MPP+ *versus* Ctrl, Ctrl + UO, MPP+ + UO. $^{\dagger}P<0.05$ Ctrl + UO or MPP+ + UO *versus* Ctrl

ischemia, and oxidative stress.[17,20] Our data indicate that chronic MPP+ exposure not only inhibited basal mitochondrial respiration, but also diminished the RC. Notably, injury combined with inhibition of ERK1/2 activation resulted in a greater RC than observed basally in uninjured cells, suggesting a biogenesis-related adaptation.

Although a single low dose of MPP+ was sufficient to inhibit oxygen consumption (Supplementary Figure S3B), presumably through direct inhibition of complex I activity, it was insufficient to cause either mitochondrial translation deficits or cell death. With repeated, chronic exposures, a significant decrease in the expression of mitochondrial respiratory complex proteins, particularly complex I, IV, and III subunits, contributed to a more permanent loss of respiratory function. These data indicate that additional cell biological mechanisms may be more important to MPP+ toxicity than simply its direct, immediate effect on complex I activity. In addition to autophagy and biogenesis, as observed in this study, microtubule-dependent trafficking could also impact functional levels of mitochondria in neurons, and several complex I inhibitors have been shown to impair microtubule function.[15]

Blocking different protease degradation pathways partially prevented the MPP+-induced decreases in mitochondrial respiratory complex proteins, suggesting that degradation is only one of the mechanisms leading to decreased expression levels. Indeed, after 1 week of MPP+ treatment, there was substantial inhibition of mtDNA-, but not nuclear DNA-, encoded protein synthesis. It is possible that decreases in expression of mtDNA-encoded proteins can impair the overall stability of mitochondrial complexes, resulting in enhanced degradation of nuclear DNA-encoded subunits. Although we didn't observe notable changes in nuclear DNA-encoded protein synthesis, nor were there significant changes in the mRNA levels of several nuclear-encoded subunits, the possibility of post-transcriptional or translational regulation of these proteins remains.

Increasing evidence indicates that ERK1/2 signaling has a central role in regulating mitochondrial function.[21,22] ERK1/2 activation leads to the loss of mitochondrial membrane potential and mitochondrial swelling in renal proximal tubular cells,[23] promotes ROS production and mitochondrial calcium elevations in ischemia,[24] and increases Bax protein expression and release of cytochrome *c*.[25] The degree of mitophagy elicited by ERK activation is directly correlated with its mitochondrial localization.[2] As with acute exposures to MPP+ or 6-OHDA,[2,4] ERK1/2 was activated, albeit to a lower level, in the chronic MPP+ model.

It is known that the effects of ERK signaling in mediating multiple cellular functions are related not only to the magnitude of activation, but also to subcellular compartmentalization and temporal patterns of activation.[26] In the chronic MPP+ model, MPP+ was administrated three times per week

for 2 weeks and caused multiple cycles of periodic activation. This pattern of ERK activation might be associated with distinct effects on regulating mitochondrial turnover versus biogenesis between acute and chronic MPP^+ models, and explain why multiple administrations of MPTP are typically needed to elicit parkinsonian injury in mice. At this point, it is unknown whether the effects of ERK on mitochondrial biogenesis is mediated through cytoplasmic, nuclear or mitochondrial signaling, as ERK is known to traffic to each of these compartments with different temporal patterns of activation.

In addition to its previously described role in promoting mitophagy,[2] the current study reveals a novel role for ERK1/2 in modulating mitochondrial protein synthesis (Figure 7). Both effects would synergize in reducing levels of functional mitochondria. Studies in other cell types implicate ERK1/2 in promoting glycolytic metabolism to provide intermediates compatible with rapid growth,[27] while decreasing mitochondrial function.[22] Although decreases in mitochondrial biogenesis may confer growth advantages for transformed cells, the loss of mitochondrial content likely contributes to the toxic effects of MPP^+ in neuronal cells. Notably, protection afforded by U0126, which inhibited mitophagy as well as reversing the biogenesis deficit, was much more complete than inhibiting degradation alone. Moreover, even when ERK1/2 inhibition was delayed to the second week of MPP^+ treatments following development of significant mitochondrial injury, there was restoration of mitochondrial structure and function, indicating a key role for reparative mitochondrial biogenesis in determining successful adaptation to chronic intoxication.

Mitochondrial biogenesis is regulated by PGC-1α, NRF-1, and TFAM.[28] TFAM is responsible for initiating synthesis of mtDNA-encoded respiratory chain proteins. TFAM knockout mice exhibit respiratory chain deficits and reduced mtDNA in midbrain DA neurons,[29] whereas overexpression of TFAM elicits an increase in mtDNA and mitochondrial respiratory chain proteins.[30] We found that low dose, repetitive exposures to MPP^+ significantly decreased TFAM protein expression, reversed by co-treatment with U0126- or ERK1/2-targeted siRNA. Although siRNA knockdown of the mitochondrial LON peptidase 1 partially restored TFAM and mitochondrial respiratory protein levels, the more complete reversal observed with U0126 implicate additional mechanisms, potentially related to protein synthesis. Depending on the cellular context, ERK1/2 may either destabilize[31] or stabilize[32] mRNA species. Thus, the effects of ERK1/2 inhibition on biogenesis may depend upon whether basal or injury-stimulated contexts are studied. U0126 shows no basal effects on TFAM or mitochondrial respiratory protein levels, whereas showing striking effects in reversing the MPP^+-induced changes in protein translation and degradation. The ability of overexpressed TFAM to reverse the MPP^+-induced decreases in mitochondrial respiratory complex proteins confirmed the importance of TFAM modulation in chronic MPP^+ toxicity.

Although the total level of PGC-1α was not affected by chronic MPP^+, a decreased mitochondrial localization of PGC-1 α was observed. PGC-1α is not only located in the nucleus, but also in the mitochondria where it interacts with TFAM to regulate mitochondrial biogenesis.[18] Thus, altered localization of PGC-1α may cooperate with the loss of TFAM expression to impair mitochondrial biogenesis. Inhibiting ERK1/2 activation also restored mitochondrial distribution of PGC-1α. Although there were no changes in NRF-1 expression observed in our chronic MPP^+ setting, the possibility of functional alterations due to altered phosphorylation remains.[33]

MPP^+ sensitivity in cells is correlated with DAT expression and inversely correlated with expression of vesicular monoamine transporter 2 (VMAT2).[34,35] Repeated administration of U0126 caused an increase in DAT and a decrease in VMAT2, indicating that the protection elicited by U0126 was not due to altered transport of MPP^+. Moreover, U0126 did not affect the kinetics of acute respiratory responses to MPP^+, and conferred protection even when administered only during the second week of toxicity. Therefore, the major protective effect of U0126 in the chronic MPP^+ model is likely to involve restoration of mitochondrial protein synthesis in conjunction with partial reduction of mitochondrial degradation.

The autophagy-lysosomal degradation pathway is recognized as a key adaptive response in the pathogenesis of many neurodegenerative diseases including PD.[36] In acute injury, autophagy-lysosomal dysfunction has been demonstrated, but the role of autophagy may be influenced by additional compensatory mechanisms in a chronic low-dose toxicity setting. Although the current data demonstrate that ERK1/2-dependent autophagic cell death is also implicated in chronic MPP^+ toxicity, there are several significant differences between acute and chronic systems. In the acute model, inhibiting MEK-ERK1/2 signaling prevents autophagy/mitophagy and reduces cell death, but has no significant effect on mitochondrial morphology[4] or mitochondrial translation (Supplementary Figure S6). In the chronic model, the MEK inhibitor not only inhibited cell death but also resulted in restoration of mitochondrial structure and function, even when applied 1 week after initiation of MPP^+ injury. This difference may be attributed to the greater capacity for repair in less severely, but chronically injured cells. In the acute model, a large percentage of mitochondria are damaged, which may exceed the ability of the cell to successfully repair/regenerate sufficient functional mitochondria. However, in the chronic MPP^+ model, the turnover of damaged mitochondria, particularly when slowed by inhibiting ERK1/2, may occur at a rate more compatible with mitochondrial biogenesis.

It is interesting that inhibition of autophagy by Atg7 siRNA also seemed to alleviate some of the mitochondrial morphological and functional abnormalities caused by MPP^+. Taken together with the U0126 data, these results suggest that blunting the robust mitochondrial degradation response induced by MPP^+, which is associated with autophagic cell death in several neuronal injury models,[2,4,37] allows for eventual structural and functional mitochondrial recovery in the context of chronic low-dose injury.

In summary, we discovered a key role for mitochondrial biogenesis in adaptation to chronic parkinsonian neuronal injury elicited by repeated administration of MPP^+ in RA-differentiated SH-SY5Y cells. These data not only strengthen a growing body of data implicating dysregulation of the autophagy-lysosome system in PD pathogenesis but

also highlight a novel role for impaired mitochondrial biogenesis in determining the outcome of autophagy induction. The ERK1/2 signaling pathway has a central role in the regulation of chronic MPP$^+$ toxicity, with effects on mitochondrial content, quality, and function. Although autophagy and mitochondrial dysfunction are implicated in both acute and chronic MPP$^+$ neurotoxin models, there were striking differences in the reversibility of mitochondrial structural and functional parameters. These data indicate that the chronic MPP$^+$ model may be particularly useful for studying mechanisms that regulate localized repair and restoration of mitochondrial function in response to damaging Parkinsonian stresses.

Materials and Methods

Cell lines and treatment. SH-SY5Y cells (ATCC, Manassas, VA, USA), maintained in antibiotic-free Advanced Dulbecco's modified Eagle's medium with 5% heat-inactivated fetal calf serum (BioWhittaker, Walkersville, MD, USA), 2 mM glutamine and 10 mM HEPES, were used at passages 30–45. Cells were plated at 3×10^4/cm^2 in 6-, 24-, 48-well plates or LabTek II coverglass chamber slides (Nalge Nunc International/Thermo Fisher, Pittsburgh, PA, USA) and treated with 10 μM retinoic acid (RA) to induce neuronal differentiation for 72 h prior to and during each experiment. RA inhibits proliferation[38] and these differentiated SH-SY5Y cells can be maintained for weeks. Cells were treated with 250 or 500 μM MPP$^+$ three times per week for up to 2 weeks. Some cultures also received bafilomycin-A (5 nM; Calbiochem, San Diego, CA, USA), 1,4-diamino-2,3-dicyano-1,4-bis[2-aminophenylthio] butadiene (U0126) (5 μM; Promega, Madison, WI, USA) or E64D (10 μM, Calbiochem). A GFP-LC3-expressing stable SH-SY5Y cell line was used to assess MPP$^+$-induced LC3 puncta formation.[2] Cell viability was measured using Alamar Blue (Trek Diagnostics, Cleveland, OH, USA), excitation 540 nm, emission 590 nm, in a Spectromax M2 microplate reader (Molecular Devices, Sunnyvale, CA, USA).

RNA interference. Cells were transfected with small interfering RNA (siRNA) targeting human Atg7, the human Atg8 homolog LC3B,[4] human ERK1 (5′-CAG CUGAGCAAUGACCAUA-3′) and ERK2 (5′-GACACAACACCUCAGCAAU-3′) (Sigma, St. Louis, MO, USA) or a control non-targeting siRNA pool (Dharmacon, Lafayette, CO, USA) at 2 days before and 3 days after the first dose of MPP$^+$. Efficacy and specificity of knockdown was assessed by western blot, confirming that siRNA-mediated knockdown of protein expression persisted for more than 10 days after the second dose of siRNA.[39]

DNA transfection. Differentiated SH-SY5Y cells transfected with pCMV6-Neo vector containing HA-tagged human TFAM, which was constructed from TFAM-tGFP plasmid (Origene, Rockville, MD, USA) by replacing the tGFP-tag sequence with an HA-tag coding sequence (5′-TACCCATACGATGTTCCAGA TTACGCTTAA-3′), were treated with chronic MPP$^+$ 48 h after transfection. In some experiments, differentiated SH-SY5Y stably expressing dominant-negative MEK1 (DN-MEK1, S217A) cloned to pBABEpuro eukaryotic expression vector (gift from Dr. CJ Marshall, Cancer Research UK, London, England) were used.

Transmission electron microscopy. Cells were fixed in 2.5% glutaraldehyde at 4 °C, processed, and photographed using a JEM 1210 transmission electron microscope (JEOL, Peabody, MA, USA) as previously reported,[4] using NIH ImageJ software to analyze mitochondrial profiles.

Fluorescence microscopy. SH-SY5Y cells fixed with 3% paraformaldehyde or methanol were probed with mouse anti-LC3 (1 : 100, Clone 2G6, Nanotools, San Diego, CA, USA) or mouse anti-human mitochondrial antigen 60KD (clone 113–1; 1 : 100; BioGenex, San Ramon, CA, USA), followed by Cy3-conjugated anti-rabbit antibody (1 : 500; Jackson Immuno-Research Laboratories, West Grove, PA, USA) or Alexa Fluor 488-conjugated antibody (1 : 500; Molecular Probes, Eugene, OR, USA), and imaged at 541/572 nm and 490/520 nm (excitation/emission), respectively.

Mitochondrial membrane potential measurement. Cells were labeled with 5,5′,6,6′-tetrachloro-1,1′,3,3′-tetraethyl benzimidazolyl carbocyanine iodide (JC-1, 5 μg/ml; Molecular Probes) for 15 min at 37 °C and rinsed with PBS. The signal intensity was measured by fluorescence well scan photometry (red, ex 535/ em 590 nm; green, ex 485/ em 530 nm) in a Spectromax M2 microplate reader (Molecular Devices), or imaged using an Olympus fluorescence microscope IX-71 (Olympus America Inc., Melville, NY, USA).

Western blot analysis and densitometry. Cells were disrupted in 0.1% Triton X-100 with protease/phosphatase inhibitors, electrophoresed through 5–15% gradient polyacrylamide gels and immunoblotted as described previously,[4] using mouse anti-phospho-ERK1/2 (1 : 1000, Cell Signaling, Beverly, MA, USA), rabbit anti-ERK1/2 (1 : 10 000, Millipore, Billerica, MA, USA), mouse anti-p110 mitochondrial protein (1 : 500; Oncogen, Boston, MA, USA), mouse anti-human mitochondrial antigen 60KD rabbit anti-human tom20 (1 : 10 000, Santa Cruz Biotechnology, Santa Cruz, CA, USA), mouse anti-pyruvate dehydrogenase E2 subunit (1 : 2000; Molecular Probes), mouse anti-LC3 (1 : 500, clone 5F10, Nanotools), rabbit anti-calnexin (1 : 4000, Calbiochem), rabbit anti-cytochrome p450 reductase (CPR, 1 : 4000, Santa Cruz), rabbit anti-ATG7 (1 : 1000, Rockland, Gilbertsville, PA, USA), Rabbit anti-HA (1 : 1000, Rockland), mouse anti-nuclear-encoded NADH-ubiquinone oxidoreductase alpha subunit 9 (NDUFA9, 1 : 1000, Abcam, Cambridge, MA, USA), MitoProfile Total OXPHOS antibody cocktail (1 : 1000, MitoSciences, Eugene, Oregon, USA), rabbit anti-mitochondrial transcription factor A (TFAM, 1 : 10 000, provided by Dr. C Cameron), rabbit anti-nuclear respiratory factor 1 (NRF-1, 1 : 5000, Abcam), rabbit anti-peroxisome proliferator-activated receptor gamma coactivator 1-alpha (PGC1α, 1 : 500, Santa Cruz), mouse anti-β-actin (1 : 10 000, Sigma), and rabbit anti-glyceraldehyde-3-phosphate dehydrogenase (GAPDH, 1 : 10 000, Abcam). Densitometry was performed using the electrophoresis documentation and analysis system 120 (Kodak, Rochester, NY, USA).

ERK1/2 activity assay. *In situ* ERK1/2 activity was assessed using the PathDetect Elk1 trans-Reporting System (Stratagene, La Jolla, CA, USA) as previous reported.[2] This system measures ERK1/2-dependent transactivation of Elk1 in cells, which drives expression of luciferase. Endogenous ERK1/2 was isolated from treated cells using the MAPK Immunoprecipitation Kinase Assay Kit (Upstate Biotechnology, NY, USA) for *in vitro* activity assay using myelin basic protein as substrate.

Mitochondrial respiration assay. Oxygen consumption rates (OCR) in living cells were analyzed at baseline and following the sequential addition of 1 μM oligomycin, 300 nM FCCP, 120 mM 2-deoxyglucose and 1 μM rotenone (final concentrations) using the XF24 Extracellular Flux Analyzer (Seahorse Bioscience, North Billerica, MA, USA). Steady-state cellular ATP concentrations were measured using the ATPLite-M luminescence assay (PerkinElmer; Waltham, MA, USA) and a Synergy 2 Multi-Mode Microplate Reader (BioTek, Winooski, VT, USA) in a black 96-well microplate in glucose-free DMEM with galactose; under these conditions cells rely on OXPHOS for ATP generation.[16]

[^{35}S]-Methonine labeling of mitochondrial translation products *in vivo*. Mitochondrial protein synthesis was assayed by [^{35}S]-methionine pulse labeling experiments.[40] Cells were washed and incubated in methionine-free and cysteine-free DMEM for 30 min, and then incubated for 5 min at 37 °C in the same medium containing 100 μg/ml of the eukaryotic translation inhibitor emetine. After the addition of 0.2 mCi (1175 Ci/mmol) [^{35}S]-methionine, the cells were incubated for 2 h. Lysates (25 μg protein) were resolved on SDS-PAGE gels, and quantified by phosphorimaging.

Statistics. All graphed data represent mean +/− S.E.M. from replicate experiments. Data were analyzed by one-way analysis of variance with post-hoc Fisher's least significant difference, two-way ANOVA or chi-square test as appropriate. Values of $P < 0.05$ were considered significant.

Conflict of Interest

The authors declare no conflict of interest.

Acknowledgements. We thank Dr. C Cameron (Pennsylvania State University) for TFAM antibodies, CJ Marshall, (Cancer Research UK, London, England) for DN-MEK1, and SJ Cherra III for his assistance with PGC-1α image analysis. This work was supported by funding from the National Institutes of Health (AG026389 and NS065789) and PA CURE (BVH).

1. Schon EA, Przedborski S. Mitochondria: the next (neurode)generation. *Neuron* 2011; **70**: 1033–1053.
2. Dagda RK, Zhu J, Kulich SM, Chu CT. Mitochondrially localized ERK2 regulates mitophagy and autophagic cell stress: implications for Parkinson's disease. *Autophagy* 2008; **4**: 770–782.
3. Cheng HC, Kim SR, Oo TF, Kareva T, Yarygina O, Rzhetskaya M *et al.* Akt suppresses retrograde degeneration of dopaminergic axons by inhibition of macroautophagy. *J Neurosci* 2011; **31**: 2125–2135.
4. Zhu JH, Horbinski C, Guo F, Watkins S, Uchiyama Y, Chu CT. Regulation of autophagy by extracellular signal-regulated protein kinases during 1-methyl-4-phenylpyridinium-induced cell death. *Am J Pathol* 2007; **170**: 75–86.
5. Plowey ED, Cherra SJ III, Liu YJ, Chu CT. Role of autophagy in G2019S-LRRK2-associated neurite shortening in differentiated SH-SY5Y cells. *J Neurochem* 2008; **105**: 1048–1056.
6. Cuervo AM, Stefanis L, Fredenburg R, Lansbury PT, Sulzer D. Impaired degradation of mutant alpha-synuclein by chaperone-mediated autophagy. *Science* 2004; **305**: 1292–1295.
7. Xilouri M, Vogiatzi T, Vekrellis K, Park D, Stefanis L. Abberant alpha-synuclein confers toxicity to neurons in part through inhibition of chaperone-mediated autophagy. *PLoS ONE* 2009; **4**: e5515.
8. Zhu JH, Guo F, Shelburne J, Watkins S, Chu CT. Localization of phosphorylated ERK/MAP kinases to mitochondria and autophagosomes in Lewy body diseases. *Brain Pathol* 2003; **13**: 473–481.
9. Higashi S, Moore DJ, Minegishi M, Kasanuki K, Fujishiro H, Kabuta T *et al.* Localization of MAP1-LC3 in vulnerable neurons and Lewy bodies in brains of patients with dementia with Lewy bodies. *J Neuropathol Exp Neurol* 2011; **70**: 264–280.
10. DeFord SM, Wilson MS, Rice AC, Clausen T, Rice LK, Barabnova A *et al.* Repeated mild brain injuries result in cognitive impairment in B6C3F1 mice. *J Neurotrauma* 2002; **19**: 427–438.
11. Chinta SJ, Andersen JK. Reversible inhibition of mitochondrial complex I activity following chronic dopaminergic glutathione depletion *in vitro*: implications for Parkinson's disease. *Free Radic Biol Med* 2006; **41**: 1442–1448.
12. Fornai F, Schluter OM, Lenzi P, Gesi M, Ruffoli R, Ferrucci M *et al.* Parkinson-like syndrome induced by continuous MPTP infusion: convergent roles of the ubiquitin-proteasome system and alpha-synuclein. *Proc Natl Acad Sci USA* 2005; **102**: 3413–3418.
13. Mizushima N, Yoshimori T. How to interpret LC3 immunoblotting. *Autophagy* 2007; **3**: 542–545.
14. Pattingre S, Bauvy C, Codogno P. Amino acids interfere with the ERK1/2-dependent control of macroautophagy by controlling the activation of Raf-1 in human colon cancer HT-29 cells. *J Biol Chem* 2003; **278**: 16667–16674.
15. Choi WS, Palmiter RD, Xia Z. Loss of mitochondrial complex I activity potentiates dopamine neuron death induced by microtubule dysfunction in a Parkinson's disease model. *J Cell Biol* 2011; **192**: 873–882.
16. Rossignol R, Gilkerson R, Aggeler R, Yamagata K, Remington SJ, Capaldi RA. Energy substrate modulates mitochondrial structure and oxidative capacity in cancer cells. *Cancer Res* 2004; **64**: 985–993.
17. Yadava N, Nicholls DG. Spare respiratory capacity rather than oxidative stress regulates glutamate excitotoxicity after partial respiratory inhibition of mitochondrial complex I with rotenone. *J Neurosci* 2007; **27**: 7310–7317.
18. Aquilano K, Vigilanza P, Baldelli S, Pagliei B, Rotilio G, Ciriolo MR. Peroxisome proliferator-activated receptor gamma co-activator 1alpha (PGC-1alpha) and sirtuin 1 (SIRT1) reside in mitochondria: possible direct function in mitochondrial biogenesis. *J Biol Chem* 2010; **285**: 21590–21599.
19. Chang JS, Huypens P, Zhang Y, Black C, Kralli A, Gettys TW. Regulation of NT-PGC-1alpha subcellular localization and function by protein kinase A-dependent modulation of nuclear export by CRM1. *J Biol Chem* 2010; **285**: 18039–18050.
20. Flynn JM, Choi SW, Day NU, Gerencser AA, Hubbard A, Melov S. Impaired spare respiratory capacity in cortical synaptosomes from Sod2 null mice. *Free Radic Biol Med* 2011; **50**: 866–873.
21. Monick MM, Powers LS, Barrett CW, Hinde S, Ashare A, Groskreutz DJ *et al.* Constitutive ERK MAPK activity regulates macrophage ATP production and mitochondrial integrity. *J Immunol* 2008; **180**: 7485–7496.
22. Nowak G, Clifton GL, Godwin ML, Bakajsova D. Activation of ERK1/2 pathway mediates oxidant-induced decreases in mitochondrial function in renal cells. *Am J Physiol Renal Physiol* 2006; **291**: F840–F855.
23. Zhuang S, Kinsey GR, Yan Y, Han J, Schnellmann RG. Extracellular signal-regulated kinase activation mediates mitochondrial dysfunction and necrosis induced by hydrogen peroxide in renal proximal tubular cells. *J Pharmacol Exp Ther* 2008; **325**: 732–740.
24. Sucher R, Gehwolf P, Kaier T, Hermann M, Maglione M, Oberhuber R *et al.* Intracellular signaling pathways control mitochondrial events associated with the development of ischemia/ reperfusion-associated damage. *Transpl Int* 2009; **22**: 922–930.
25. Zhang CL, Wu LJ, Zuo HJ, Tashiro S, Onodera S, Ikejima T. Cytochrome c release from oridonin-treated apoptotic A375-S2 cells is dependent on p53 and extracellular signal-regulated kinase activation. *J Pharmacol Sci* 2004; **96**: 155–163.
26. Ebisuya M, Kondoh K, Nishida E. The duration, magnitude and compartmentalization of ERK MAP kinase activity: mechanisms for providing signaling specificity. *J Cell Sci* 2005; **118**(Pt 14): 2997–3002.
27. Marko AJ, Miller RA, Kelman A, Frauwirth KA. Induction of glucose metabolism in stimulated T lymphocytes is regulated by mitogen-activated protein kinase signaling. *PLoS ONE* 2010; **5**: e15425.
28. Scarpulla RC. Transcriptional paradigms in mammalian mitochondrial biogenesis and function. *Physiol Rev* 2008; **88**: 611–638.
29. Ekstrand MI, Terzioglu M, Galter D, Zhu S, Hofstetter C, Lindqvist E *et al.* Progressive parkinsonism in mice with respiratory-chain-deficient dopamine neurons. *Proc Natl Acad Sci USA* 2007; **104**: 1325–1330.
30. Iyer S, Thomas RR, Portell FR, Dunham LD, Quigley CK, Bennett JP Jr.. Recombinant mitochondrial transcription factor A with N-terminal mitochondrial transduction domain increases respiration and mitochondrial gene expression. *Mitochondrion* 2009; **9**: 196–203.
31. Sato M, Shegogue D, Hatamochi A, Yamazaki S, Trojanowska M. Lysophosphatidic acid inhibits TGF-beta-mediated stimulation of type I collagen mRNA stability via an ERK-dependent pathway in dermal fibroblasts. *Matrix Biol* 2004; **23**: 353–361.
32. Zhai B, Yang H, Mancini A, He Q, Antoniou J, Di Battista JA. Leukotriene BBLT receptor signaling regulates the level and stability of cyclooxygenase-2 (COX-2) mRNA through restricted activation of Ras/Raf/ERK/p42 AUF1 pathway. *J Biol Chem* 2010; **285**: 23568–23580.
33. Piantadosi CA, Suliman HB. Mitochondrial transcription factor A induction by redox activation of nuclear respiratory factor 1. *J Biol Chem* 2006; **281**: 324–333.
34. Chen CX, Huang SY, Zhang L, Liu YJ. Synaptophysin enhances the neuroprotection of VMAT2 in MPP + -induced toxicity in MN9D cells. *Neurobiol Dis* 2005; **19**: 419–426.
35. Pifl C, Giros B, Caron MG. Dopamine transporter expression confers cytotoxicity to low doses of the parkinsonism-inducing neurotoxin 1-methyl-4-phenylpyridinium. *J Neurosci* 1993; **13**: 4246–4253.
36. Nixon RA. Autophagy in neurodegenerative disease: friend, foe or turncoat? *Trends Neurosci* 2006; **29**: 528–535.
37. Chakrabarti L, Eng J, Ivanov N, Garden GA, La Spada AR. Autophagy activation and enhanced mitophagy characterize the Purkinje cells of pcd mice prior to neuronal death. *Mol Brain* 2009; **2**: 24.
38. Simpson PB, Bacha JI, Palfreyman EL, Woollacott AJ, McKernan RM, Kerby J. Retinoic acid evoked-differentiation of neuroblastoma cells predominates over growth factor stimulation: an automated image capture and quantitation approach to neuritogenesis. *Anal Biochem* 2001; **298**: 163–169.
39. Bartlett DW, Davis ME. Insights into the kinetics of siRNA-mediated gene silencing from live-cell and live-animal bioluminescent imaging. *Nucleic Acids Res* 2006; **34**: 322–333.
40. Yang Y, Cimen H, Han MJ, Shi T, Deng JH, Koc H *et al.* NAD + -dependent deacetylase SIRT3 regulates mitochondrial protein synthesis by deacetylation of the ribosomal protein MRPL10. *J Biol Chem* 2010; **285**: 7417–7429.

Supplementary Information accompanies the paper on Cell Death and Disease website (http://www.nature.com/cddis)